In situ pulsed laser-induced thermal desorption studies of the silicon chloride surface layer during silicon etching in high density plasmas of Cl_2 and Cl_2/O_2 mixtures

C. C. Cheng, K. V. Guinn, V. M. Donnelly, and I. P. Herman[a)]
AT&T Bell Laboratories, Murray Hill, New Jersey 07974

(Received 24 February 1994; accepted 27 May 1994)

We have used laser-induced thermal desorption, combined with laser-induced fluorescence of $SiCl_{(g)}$ to study, in real time, the Si-chloride ($SiCl_{x(ads)}$) layer that is present on the surface during Si etching in a high-plasma density, low pressure Cl_2 helical resonator plasma. The $SiCl_{x(ads)}$ layer that builds up during etching contains about twice as much Cl as the saturated layer that forms when Si is exposed to Cl_2 gas. By varying the laser repetition rate we determined that the surface is chlorinated with an apparent first-order time constant of ~6 ms at 1.0 mTorr, and 20 ms at 0.3 mTorr. Therefore in the plasma at pressures above ~0.5 mTorr, the $SiCl_{x(ads)}$ layer reaches saturated coverage on a time scale that is short compared to the time required to etch one monolayer (40 ms). From the weak dependence of the $SiCl_{x(ads)}$ layer coverage on discharge power (0.2–1 W/cm^3), substrate bias voltage (from 0 to −50 V dc), and pressure (0.5–10 mTorr), we conclude that ion flux, and not neutral etchant flux (i.e., Cl and Cl_2), limits the etch rate, even in a low pressure, high-charge-density plasma. The chemically enhanced Cl_2^+ sputtering yield is 0.38 at an ion energy of 50 eV and 0.60 at 125 eV. Because of the relatively low neutral-to-ion flux ratios (~2:1 at the lowest pressures) compared to reactive ion etching conditions, a substantial portion of the chlorine needed to form volatile products can be provided by the impinging ions. The $SiCl_{x(ads)}$ layer does not change appreciably (<10% decrease in Cl coverage) after the plasma is extinguished and the gas is pumped away. Consequently, post-etching surface analysis measurements on samples that are transferred under ultrahigh vacuum to an analysis chamber provide information on the surface as it was during etching. The $SiCl_{x(ads)}$ coverage and etch rate decreases with increasing addition of O_2 to Cl_2, due to the competition for adsorption sites by O.

I. INTRODUCTION

Lower pressure, higher charge density plasmas are increasingly being investigated and implemented to achieve faster etch rates, better selectivities, and improved control over etched profiles. Along with the higher fluxes of ions, these conditions produce lower ion energies and lower fluxes of neutral species. Although the percent dissociation of feed gases is, in general, larger for higher plasma densities, the lower pressures usually lead to lower fluxes of radical species. Diagnostic studies are needed to determine what limits etching rates, profile control, uniformity, etc. under these conditions, so future research and development can be properly directed. To understand the role of the supply of neutral species to the surface, a diagnostic technique is needed to measure adsorbate coverages on the surface during etching.

Identifying these adsorbates in real time is a difficult task. Standard surface analysis techniques such as Auger electron spectroscopy (AES), x-ray photoelectron spectroscopy (XPS), and electron energy loss spectroscopy (EELS) cannot be applied in the presence of charged particles, and at the high pressures used in etching and deposition processes (1–1000 mTorr). Several optical techniques have recently been applied to this problem. Ellipsometry can provide some information on the presence of adsorbates during etching.[1–3] Interpretations depend on modeling, however, and chemical analysis is not possible. Surface-based photoemission[4] and photoluminescence[5] have been applied to plasma processing. While these techniques are very sensitive to the presence of certain adsorbates, and for photoluminescence during III-V compound semiconductor plasma processing to the onset of surface damage, they are hard to quantify and give no chemical identification. Infrared (IR) absorption, and in particular Fourier transform IR (FTIR), can provide chemical identification, and has been used to probe surfaces during plasma processing.[6] However, special total-internal-reflection substrates are needed for high sensitivity, and interferences from substrate absorption bands limit this technique. In addition, fast time response is not possible because of the signal averaging necessary to extract the weak absorbances.

None of these techniques can provide the quantitative chemical identification possible with AES and XPS. Consequently, many efforts have involved preparing samples in the processing environment, and then transferring the sample to an ultrahigh vacuum (UHV) chamber without air exposure.[7–16] In one such recent XPS study, we determined the composition and coverage of adsorbates that were present on polycrystalline Si masked with photoresist after etching in a high-density, low pressure helical resonator Cl_2 plasma.[16] One question in these post-processing analysis studies is whether the results are representative of the surface under steady-state processing conditions in the presence of gases, and, in plasma processes, charged particle bombardment.

Recently, we used laser-induced desorption, combined

[a)]Also with the Department of Applied Physics and the Columbia Radiation Laboratory, Columbia University, New York, NY 10027.

 0734-2101/94/12(5)/2630/11/$1.00

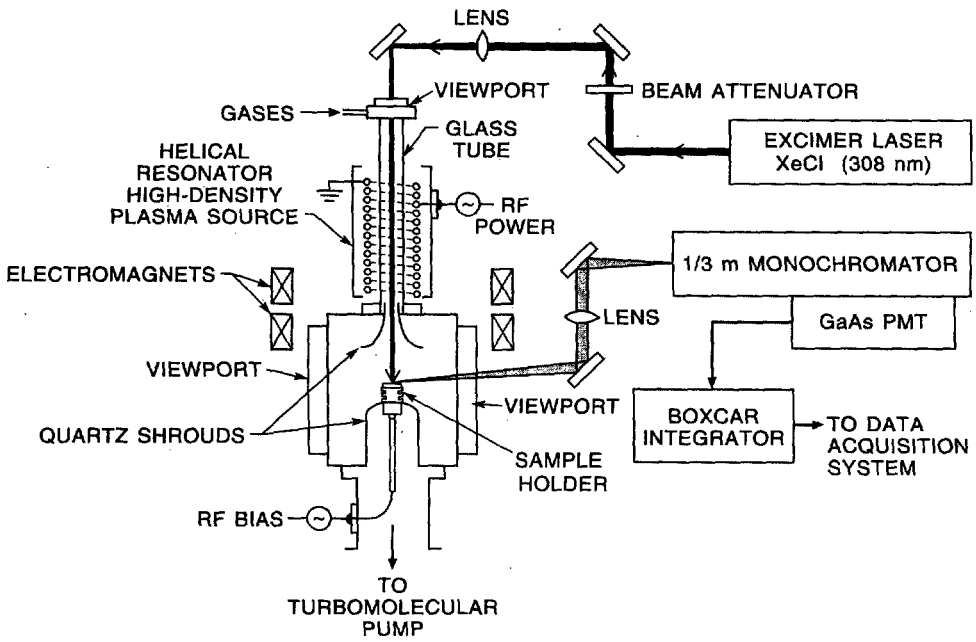

FIG. 1. Schematic depiction of the apparatus used for laser induced thermal desorption/emission measurements during plasma etching. The vacuum transfer chamber and UHV/XPS chamber are not shown.

with laser-induced fluorescence,[17] to show that the Si-chloride layer that is present during etching in this plasma[16] is stable after the plasma is extinguished; its thickness decreases by <10% in the time needed to transfer samples to the analysis chamber and perform subsequent XPS measurements. In the present study, we have used this technique to measure, in real time, the dependence of the chlorine content of this layer on discharge power, substrate bias voltage, pressure, and added oxygen. The transient behavior of the layer thickness has also been determined as etching conditions are changed.

II. EXPERIMENTAL PROCEDURE

The plasma reactor, optical spectrometer, and excimer laser used in this study are depicted in Fig. 1, and have been described in detail elsewhere.[16–20] The plasma reactor is connected to an ultrahigh vacuum (UHV) XPS analysis chamber[16] (not shown in Fig. 1). The plasma reactor[16] consists of a 6 in. stainless-steel cube, forming a "downstream" region, with a 2 in. diam vertical glass tube that is connected to the top of the cube and serves as the "upstream" discharge region. A 4 in. diam 16-turn quarter-wave helical coil and 8 in. diam ground shield surround this glass tube, forming the helical resonator source.[21–23] A 100 G solenoid magnet concentrically surrounds the lower part of the ground shield, and a second 100 G magnet concentrically surrounds the downstream region. The discharge was operated at a pressure of 1.0 mTorr at a total flow of 5.5 standard cubic cm per min (sccm). In most cases, pure Cl_2 was used; Cl_2/O_2 gas mixtures were also investigated. In one set of experiments with pure Cl_2, the pressure was varied from 0.2 to 20 mTorr. The flow rate was reduced to 1 sccm to obtain pressures below 1 mTorr. Pressures were measured with a capacitance manometer and the reactor was pumped from below with a 240 ℓ/s turbomolecular pump.

The helical resonator plasma source was operated at a radio frequency (rf) of 11.21 MHz and a net power of 280 W, measured with in-line power meters. In one set of experiments, the power was varied from 5 to 500 W. The substrate stage was biased with a second rf voltage (14.5 MHz), providing dc bias voltages of 0 (grounded stage) to −120 V. Electrical measurements were made with a Langmuir probe (PMT Fastprobe). At 1 mTorr, the plasma potential was 50 V, independent of dc bias. An electron density of 1.5×10^{11} cm^{-3} was measured for an Ar plasma under the same pressure and power conditions. Saturated ion current density (I_{sat}) measurements were performed as a function of power, bias voltage, and pressure. Under the conditions used for many of the measurements presented below (280 W helical resonator power, 1 mTorr Cl_2 pressure), I_{sat}=6.3 mA/cm^2 (independent of substrate bias voltage), which corresponds to a positive ion flux of 3.9×10^{16} cm^{-2} s^{-1}. A Cl_2 plasma gas temperature of 500±50 K was estimated by adding a small amount of N_2 to the discharge (1%–20%), and measuring the "rotational temperature" of the N_2 second positive emission.[24] Several investigations at higher pressures have shown that this provides an accurate measure of the translational temperature of the main plasma gas.[25–27] Within the quoted uncertainty, the gas temperature was independent of $\%N_2$, pressure (0.3 and 1.0 mTorr), and the length of time that the plasma was on. At 10 mTorr Cl_2 pressure, the gas temperature was somewhat higher (650±50 K). The mean free path at a Cl_2 pressure of 10 mTorr is ~1 cm, so N_2 will undergo several collisions in the discharge zone and equilibration between rotational and translational energy is reason-

able. Below 1 mTorr, however, the mean free path is >10 cm and therefore exceeds the dimensions of the discharge. Consequently, the rotational temperature may differ from the translational temperature at the lower pressures.

The substrates used in the laser-induced desorption experiments were *n*-type Si(100) (P-doped, 5–50 Ω cm). In etch rate measurements, 5000 Å thick, undoped polycrystalline Si films deposited on 1000 Å of SiO_2 on Si(100) were used. The poly-Si etch rate was measured interferometrically with a 6734 Å AlGaAs laser.[16] Cleaved samples (~1.5×1.5 cm) were clamped to a 1 in. diam stainless-steel sample holder that can be transferred from the etching chamber under UHV through a load-lock chamber to the analysis chamber. The top of the stainless-steel sample holder was covered with a 1 in. diam Si wafer that was bonded with indium solder.

The excimer laser (Lambda Physics Model EMG 203) was operated at 308 nm (XeCl) and delivered a maximum of 230–150 mJ/pulse between 1 and 80 Hz, respectively. The beam reflected from three mirrors and passed through two lenses and a quartz viewport before irradiating the surface at normal incidence, with about half of the initial pulse energy. The lenses were used to reduce the beam size to a rectangular spot of 2.6×6.2 mm at the substrate surface. Quartz flats were inserted into the beam to further attenuate it to the desired fluence.

Laser-induced fluorescence (LIF) was monitored at a mean angle of ~75° with respect to the laser beam. Fluorescence was dispersed with a 0.35 m focal length scanning monochromator and detected with a GaAs photomultiplier tube. Entrance and exit slits widths of either 50 or 150 μm were used, giving a resolution of 1.2 or 3.5 Å, respectively. Imaging optics were used to focus light from the near-surface region (0–4 mm above the surface) onto the entrance slit of the monochromator. A boxcar integrator (SRI Model SR250/SR280) was used to detect the transient signals induced by the ~15 ns laser pulses. The boxcar gate width was 1 μs, long enough to integrate over the entire signal pulse. The signals were recorded with a computer.

III. RESULTS AND DISCUSSION

A. Nature of the laser-induced fluorescence signal

With the collection optics imaged on the near-surface region, LIF was detected during Cl_2 plasma etching when the laser irradiated the surface at fluences above ~0.2 J/cm^2. The fluorescence spectrum (Fig. 2) indicates that the emitter is $SiCl(B\ ^2\Sigma^+)$,[24,28–30] excited in the gas phase by a fortuitous resonance at 308 nm with the transitions:

$$B\ ^2\Sigma^+(v'=0) \leftarrow X\ ^2\Pi_r(v''=3,4). \quad (1)$$

Both spin-orbit components ($r=1/2$ and 3/2) are excited. The weaker emission between 2730 and 2910 Å is likely due to excitation of $v'=1$ and 2 from $v''=5$ and 6.

The fluence and spatial dependencies indicate that the signal is a result of laser-induced thermal desorption of $SiCl_{(g)}$.[17,31–35] At fluences below ~0.2 J/cm^2, no fluorescence is observed, indicating that $SiCl_{(g)}$ LIF is not from excitation of SiCl [$X\ ^2\Pi_r(v''=3,4)$] that could be present in the plasma as a primary product of plasma etching, or could be formed by electron-impact dissociation of the $SiCl_{2(g)}$ or $SiCl_{4(g)}$ products of plasma etching. This mechanism would exhibit a LIF signal that would have a linear dependence on laser fluence (or even sublinear if the transition were near saturation). Instead, above the apparent threshold near 0.2 J/cm^2, the signal increases rapidly to a saturation level near 0.6 J/cm^2.[17] This fluence dependence is a strong indication of a thermal desorption process resulting from pulsed laser-induced transient heating of the Si surface. Additional support for this mechanism is found in the spatial dependence of the signal intensity. When the collection optics were moved to detect fluorescence integrated over a volume extending 1–14 mm directly above the irradiated region of the surface, nearly excluding this near-surface region from view, the LIF signal was reduced by a factor of ~40. This is expected for a product like $SiCl_{(g)}$ that (1) desorbs as a result of laser irradiation of the surface, (2) is excited by the temporal tail of the same 15 ns long laser pulse, and (3) fluoresces in a time so short (10 ns)[36] that it moves only a small distance (<0.1 mm) from the surface before emitting.

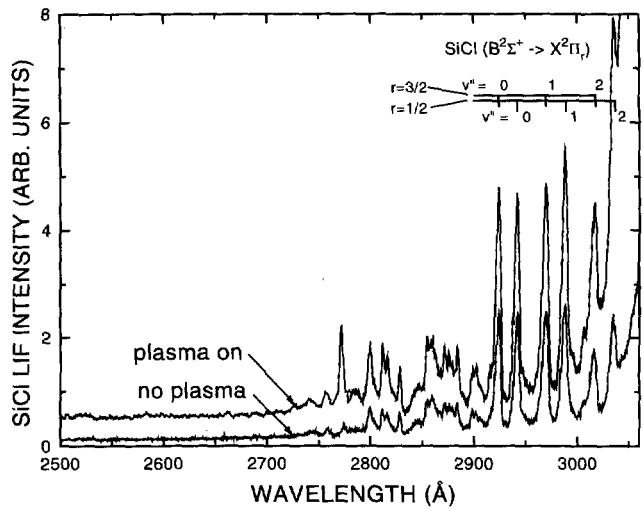

FIG. 2. Spectra recorded during etching of Si(100). $P_{Cl_2}=1.0$ mTorr, Cl_2 flow rate=5.5 sccm, laser repetition rate=10 Hz, fluence=0.50 J/cm^2. Top trace: LD-LIF spectrum during plasma etching. Helical resonator power =280 W, substrate bias voltage=−34 V dc. Bottom trace: LD-LIF spectrum with no plasma, due to laser-induced etching. The features at 2772 Å are artifacts caused by diffraction of laser light in the monochromator.

This laser desorption-laser induced fluorescence (LD-LIF) process can also be distinguished from laser desorption-plasma induced emission (LD-PIE) by its spatial and temporal dependence. LD-PIE results from an enhancement of the ordinary emission excited by electron impact or other energetic processes. This enhancement occurs when laser-induced thermal desorption causes a transient increase in etching product concentrations in the plasma. LD-PIE was also observed during Si etching in a Cl_2 plasma by collecting light from a region several mm above the sample.[17] These desorption products are excited by the PIE process as they enter the plasma, causing a transient signal. This process is discussed in more detail elsewhere.[17]

A $SiCl_{(g)}$ LD-LIF signal was also observed when the

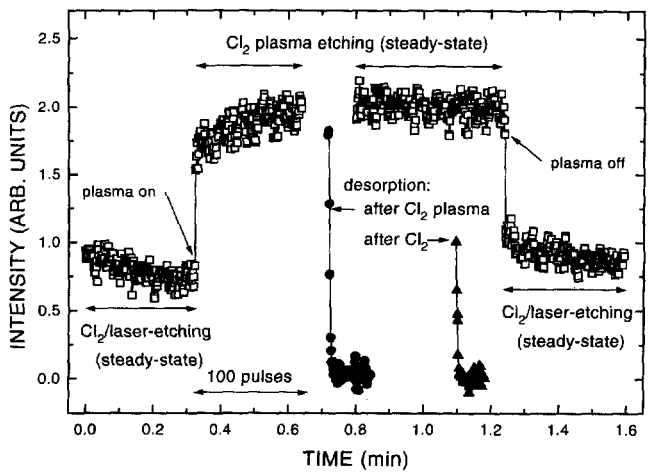

FIG. 3. LIF intensity of laser-desorbed SiCl (2924 Å) as a function of time. The open squares show steady-state laser-induced etching of Si by Cl_2, and then etching with the plasma suddenly turned on (at 0.33 min) and off (at 1.25 min). Laser repetition rate=5 Hz. Other conditions are the same as for Fig. 2. The solid symbols show the time dependence of desorbed SiCl after chlorination with the plasma off (▲) and on (●), and subsequent pump-down. The times for these last two traces were offset so that they were near the respective steady-state traces.

plasma was off, due to laser-induced etching in the presence of Cl_2. This fluorescence spectrum, also shown in Fig. 2, is virtually identical to that observed during plasma etching, except that the intensity is about half as large. The fluence dependence for this process is similar to that observed for LD-LIF during plasma etching, except that the threshold fluence is higher (~0.35 J/cm^2). Aliouchouche *et al.*[31] have reported desorption of $SiCl_{(g)}$ accompanying XeCl excimer laser-induced etching of Si(100) in a Cl_2 ambient. Using time-of-flight mass spectrometry, Boulmer *et al.*[32–34] have shown that $SiCl_{(g)}$ is a major product of XeCl excimer laser induced etching of Si(100) by Cl_2.

The time dependence of the formation of the silicon chloride ($SiCl_{x(ads)}$) layer that gives rise to the $SiCl_{(g)}$ LD-LIF signal was investigated. The monochromator was set to a wavelength of intense emission (2924 Å), and the signal was recorded for every laser pulse as a function of time. Background measurements were obtained by stopping the Cl_2 flow and evacuating the reactor to a pressure (P) of $\sim 1\times10^{-7}$ Torr. A typical series of measurements is shown in Fig. 3. Similar measurements have been presented elsewhere.[17]

The signal observed during laser-induced etching (plasma off) remained nearly constant for minutes (two portions of which are shown in Fig. 3) as the sample was exposed to several thousand laser pulses. In some cases, the laser was first blocked and then the Cl_2 was pumped away ($P\sim 1\times10^{-7}$ Torr). When the laser shutter was opened, a LD-LIF signal was observed from $SiCl_{(g)}$ that decayed to baseline within ~5 pulses. A typical decay is included in Fig. 3, with its arbitrary starting time shifted to facilitate comparison with the steady-state laser-induced etching signal. Signals decayed exponentially over a tenfold decrease, with a "lifetime" ($1/e$) of 1.0±0.1 laser pulses at a fluence of 0.5 J/cm^2. The area under these decay curves is proportional to the $SiCl_{x(ads)}$ layer thickness (and/or coverage), since most of the layer has been removed by the time the LD-LIF signal has decayed to the base line (see discussion below). Note that the signal intensity with the first laser pulse is nearly equal to the steady-state level observed during laser-induced etching, indicating that the thickness of the $SiCl_{x(ads)}$ layer changes little (<10%) for many minutes after stopping the process.

The $SiCl_{x(ads)}$ layer formed during laser-induced etching is likely to be similar to that formed in UHV studies of clean Si(100) (2×1). Any oxide or carbon impurities should be removed in the etching process. The surface is heated near, or to the melting point on each pulse. A similar laser-annealing process has been reported to prepare a well-ordered (2×1) surface.[37] Since the surface is hot for only a short time, most of the dosing occurs when the sample is near room temperature. When clean Si(100) (2×1) is dosed with Cl_2 in UHV at room temperature, a saturated coverage of 4.8×10^{14} cm^{-2} of Cl is found.[38,39] The $SiCl_{x(ads)}$ layer is believed to be composed of ~70% $SiCl_{(ads)}$ and ~30% unchlorinated Si.[38] Photoemission measurements show that the Si(100) surface is covered with about one monolayer (ML) of $SiCl_{(ads)}$, a small amount of $SiCl_{2(ads)}$ (0.1 ML), and no detectable $SiCl_{3(ads)}$.[40]

When the plasma was turned on while steady-state laser-induced etching was in progress, the $SiCl_{(g)}$ LIF signal immediately doubled [within one laser pulse at 5 Hz (see Fig. 3)], and then remained constant for at least several minutes. The converse is also true; when the plasma was turned off, the signal quickly droped by a factor of 2 (see the trace on the far right-hand side of Fig. 3). The increase in signal with the plasma on is partly due to the more weakly bound $SiCl_{x(ads)}$ layer that forms during plasma etching[17,41] and desorbs at a lower temperature, and hence lower fluence as described above. However, the fluence was high enough in the measurements presented in Fig. 3 (and the following figures) that both the plasma-on and plasma-off measurements were near saturation. Consequently, the predominant reason for the increase in the $SiCl_{(g)}$ LD-LIF signal when the plasma is turned on is that the $SiCl_{x(ads)}$ layer present during plasma etching is thicker and/or more highly chlorinated (i.e., x closer to 2) than the layer formed by exposing clean Si(100) to Cl_2. A more highly chlorinated layer is supported by XPS measurements described below.

In the last trace shown in Fig. 3, the laser was blocked and the plasma left on for a few seconds to form a fresh plasma-exposed surface, and then the plasma was extinguished and the Cl_2 was pumped away ($P\sim 1\times10^{-7}$ Torr). When the laser shutter was opened, the $SiCl_{(g)}$ LD-LIF signal intensity decayed exponentially to base line with a lifetime of 1.2±0.1 pulses, similar to what was found in laser-induced etching. The area under these decay curves is 2.2 times that of the decay curves described above that were recorded after exposure to Cl_2 with no plasma. This suggests that the $SiCl_{x(ads)}$ plasma-exposed layer is about twice the thickness or has double the chlorine content, i.e., a coverage of 1.0×10^{15} Cl/cm^2, provided that most of the product has been removed at base line (see discussion below). In addition, the signal intensity for the first pulse (after pumping away the Cl_2) was

found, on average, to be nearly equal to the signal observed for steady-state plasma etching (Fig. 3), indicating that the thickness or composition of the $SiCl_{x(ads)}$ layer present in plasma etching does not change appreciably (<10% decrease in signal after 5 min) when the plasma is extinguished and the Cl_2 is pumped away. Consequently, XPS measurements carried out after etching and then transferring the sample under vacuum to the analysis chamber[16] are representative of the surface present during etching.

B. Supportive XPS measurements

XPS measurements were made to quantify the Cl coverages under steady-state laser-induced etching and plasma etching conditions. Samples were etched with the laser only, the laser was blocked, the Cl_2 flow was stopped and the reactor was evacuated to $\sim 10^{-6}$ Torr. The samples were then transferred under vacuum to the UHV chamber. A $Cl(2p)/Si(2p)$ signal intensity ratio of 0.60 was observed. This then corresponds to 4.8×10^{14} Cl/cm^2, which is the saturation coverage that has been reported for clean Si(100) (2×1) dosed with Cl_2 at room temperature.[38] Next, plasma-etched samples were prepared and then transferred to the XPS chamber. A $Cl(2p)/Si(2p)$ ratio of 1.0 was observed, both in regions far from the laser beam and in the region irradiated by the laser, provided that the laser was blocked before the plasma was extinguished. Since the $1/e$ escape depth for electrons with a kinetic energy of 1388 eV is ~10 Å at a takeoff angle of 30°, the $Si(2p)$ signal comes mainly from the subsurface Si substrate. We estimate that the presence of 5×10^{14} Cl/cm^2 will attenuate this $Si(2p)$ signal by about 10%. Therefore the presence of an *additional* 5×10^{14} Cl/cm^2 on plasma-exposed surfaces will attenuate the $Si(2p)$ signal by an additional 10% over the attenuation of the $Si(2p)$ signal on laser-etched samples. Consequently, the ratio of Cl coverages on plasma-etched versus laser-etched samples is $1.0/(0.9\times0.60)$ or 1.9. This is close to the ratio of 2.2 observed for the integrated $SiCl_{(g)}$ LD-LIF signals on plasma-etched and laser-etched samples, and to the twofold increase in the steady-state signal when the plasma is suddenly turned on after laser-induced etching is established. Consequently, the $SiCl_{(g)}$ LD-LIF signals are a quantitative relative measure of Cl coverage.

After plasma etching without laser irradiation, high resolution XPS measurements were made of the $Si(2p)$ peak to determine the nature of the $SiCl_{x(ads)}$ layer. A sample spectrum is shown in Fig. 4 for Si(100); indistinguishable results were obtained for undoped poly-Si. The presence of multiple Si-chloride species is evident as a structured tail extending 3 eV above the binding energy of the strong bulk Si peak at 99.4 eV. Whitman *et al.*[42] have used soft x rays from a synchrotron source to characterize Si(111) surfaces after dosing with Cl_2 in UHV. They found three peaks shifted by 0.88, 1.65, and 2.72 eV from the bulk Si peak and assigned them to $SiCl_{(ads)}$, $SiCl_{2(ads)}$, and $SiCl_{3(ads)}$, respectively. Consequently, we fit four peaks to the spectrum observed in the present study. The nonlinear least-squares fit yielded binding energy shifts (relative to bulk Si) of 0.74, 1.81, and 2.93 for the respective Si chlorides, in excellent agreement with the results of Whitman *et al.*[42] The area ratios of these three

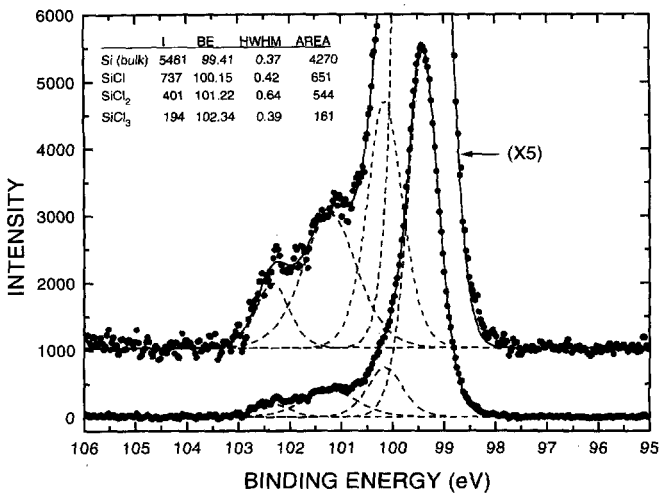

FIG. 4. $Si(2p)$ XPS spectrum for Si(100) after etching in a Cl_2 plasma, without laser irradiation. The $2p$ 1/2 component has been removed, assuming a spin-orbit splitting of 0.61 eV and a 1/2:3/2 intensity ratio of 0.52:1 (Ref. 42). The photoelectron takeoff angle was 20° with respect to the surface plane. The plasma conditions are listed in the caption for Fig. 2. The fit (solid line) includes four peaks (dashed lines) with 50% Gaussian/50% Lorentzian line shapes. No parameters were constrained during the iterative fitting procedure. The peak intensities (I), half-width at half-maximum (HWHM), peak binding energy (BE), and integrated peak intensities (AREA) for the four peaks are given in the table contained in the figure. The relative areas for $SiCl:SiCl_2:SiCl_3$ are 1.00:0.84:0.25.

peaks were 1.00:0.84:0.25, meaning that 71% of the chlorine on the surface is in the form of the di- and trichlorides. Because the peaks are not resolved, there is considerable uncertainty in the peak widths and thus relative proportions of $SiCl_{2(ads)}$ and $SiCl_{3(ads)}$. However, the sum of $SiCl_{2(ads)} + SiCl_{3(ads)}$ peak areas relative to $SiCl_{(ads)}$ is much more precise and so the conclusion that during exposure to the plasma most of the adsorbed Cl is present as higher Si chlorides remains unaltered.

As noted above, when Si(100) is exposed to Cl_2 in UHV, $SiCl_{(ads)}$ is the predominant species, and only a small amount of $SiCl_{2(ads)}$ is present.[40] Taken with the results of the present study, we therefore conclude that during laser-induced etching the surface is terminated mainly by $SiCl_{(ads)}$ groups, but exposure to the plasma greatly increases the coverage of $SiCl_{2(ads)}$ and $SiCl_{3(ads)}$. Since $SiCl_{(ads)}$ is converted to higher chlorides in this process, the coverage of $SiCl_{(ads)}$ is actually less on Si(100) surfaces exposed to the plasma. At first, these results seem at odds with the fact that at high laser fluences, the $SiCl_{(g)}$ LD-LIF signal with the plasma on is twice that measured with the plasma off. While plasma exposure is likely to increase the $SiCl_{2(g)}$ laser-desorption yield, apparently the rapid heating rate and high peak temperature in the LD-LIF process also cause dissociation of $SiCl_{2(ads)}$ and $SiCl_{3(ads)}$ to form $SiCl_{(ads)}$, followed by desorption of $SiCl_{(g)}$. This requires chlorination of Si below the $SiCl_{x(ads)}$ layer, which would be aided at surface temperatures near the melting point. Aliouchouche *et al.*[31] have invoked a mechanism to explain SiCl laser desorption in which adsorbed Cl diffuses into molten Si and then segregates to the surface during solidification. From the dependence on Cl_2 flux, Boul-

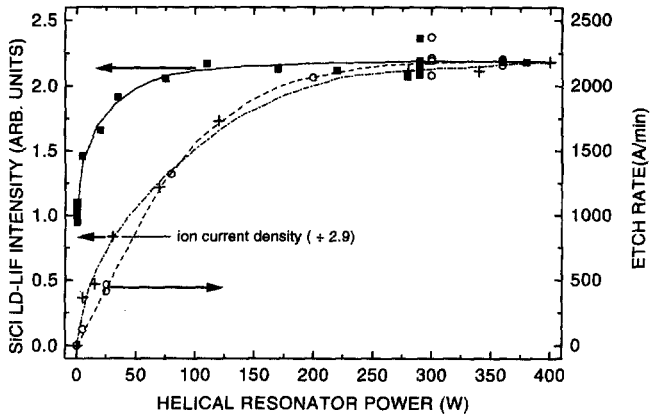

FIG. 5. SiCl LD-LIF signal intensity (—■—), etch rate (- -○- -), and I_{sat}, the saturated ion current density (- - -+- - -) vs helical resonator power. I_{sat} can be obtained by multiplying the left y-axis scale by 2.9 (i.e., I_{sat}=6.3 mA/cm^2 at 400 W). Other conditions are the same as for Fig. 2.

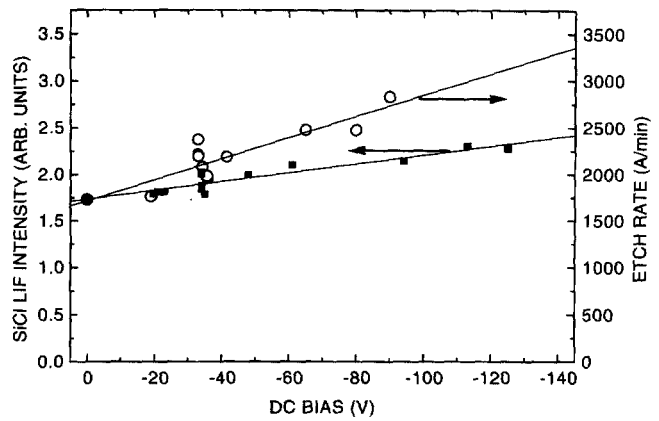

FIG. 6. SiCl LD-LIF signal intensity (■) and etch rate (○) vs substrate bias voltage. Other conditions are the same as for Fig. 2.

mer *et al.*[32] concluded that the SiCl laser-desorption yields are proportional to Cl coverage. This mechanism also suggests that the $SiCl_{(g)}$ laser-desorption yield should continue to be proportional to Cl coverage at the higher coverages obtained with plasma exposure, as observed in the present study.

Attempts were made to measure the residual Cl coverage after multiple pulse irradiation with no plasma or Cl_2 flow by quickly transferring the sample to the XPS chamber. The Cl coverage measured by XPS after this procedure varied from about half of that observed after saturated exposure to Cl_2, to only slightly less than this saturation coverage. Unfortunately, the residual Cl_2 partial pressure in the plasma reactor 30 min after etching (as high as 100% of the $\sim 7\times10^{-8}$ Torr base pressure) causes the surface to be rechlorinated in the 1 min period between this multiple pulse irradiation and transfer to the analysis chamber. Rechlorination was verified by carrying out sequential, multiple pulse LD-LIF measurements in the plasma reactor at 1 min intervals. The signal on the first pulse of each of these irradiations was much higher than the base line signal, indicating that rechlorination had occurred. Removal of most of the Cl by multiple pulse irradiation is expected from the laser-induced etching studies of Aliouchouche *et al.*[31] At fluences near saturation, they found that 80% of the Cl is removed in the first pulse. While their decays were somewhat nonexponential, they nonetheless indicated that more than 90% of the Cl was removed by multiple pulse irradiation.

C. LD-LIF parametric study of Cl_2 plasma etching of Si(100)

The $SiCl_{(g)}$ LD-LIF signal intensity observed during plasma etching is plotted in Fig. 5 as a function of power supplied to the helical resonator. The signal intensity increases rapidly above 0 W (the laser-induced etching rate level) to roughly double that value at ~100 W. Above this power, the signal (and hence the steady-state $SiCl_{x(ads)}$ layer thickness) is independent of power. Etch rates (Fig. 5) rise less steeply at low power, and saturate at a higher power. Also plotted in Fig. 5 is the saturated ion current density (I_{sat}) measured with the Langmuir probe biased at −100 V dc. The ion current saturates above 250 W at a value of 6.3 mA/cm^2, corresponding to an ion flux of 3.9×10^{16} cm^{-2} s^{-1}. The etch rate closely follows I_{sat}, suggesting that the etch rate is limited by the ion bombardment flux.

In Fig. 6, the dependence of the $SiCl_{(g)}$ LD-LIF signal is given as a function of dc self-bias voltage resulting from rf bias of the substrate holder. The dependence of the etch rate on bias is also presented in this figure. The signal increases linearly by 25% as the dc bias voltage decreases from 0 to −125 V. This could be caused by an increase in Cl coverage with increasing bias and/or by the formation of a more weakly bound species at higher bias such that the amount of product desorbed per pulse increases. To distinguish between these two mechanisms, decay measurements like the one shown in Fig. 3 were performed at four bias voltages (two each at 0, −36, −80, and −125 V dc). The integrated intensity of the decay curves (proportional to the total Cl coverage), the signal on the first laser pulse, and the steady-state signal all increase with bias in a similar way. Therefore, the increase in the steady-state $SiCl_{(g)}$ LD-LIF signal with bias is primarily a reflection of an increase in Cl coverage.

The pressure dependence of the $SiCl_{(g)}$ LD-LIF signal is shown in Fig. 7 as a function of pressure at constant power applied to the helical resonator source. The rf bias voltage was not intentionally changed, but did vary from −31 V at 0.5 mTorr to −39 V at 20 mTorr. The $SiCl_{(g)}$ LD-LIF signal increases by 7% between 0.2 (the lowest pressure at which a stable plasma could be sustained) and 1 mTorr, and then falls by 8% between 1 and 20 mTorr. This indicates that the $SiCl_{x(ads)}$ layer thickness saturates at a very low pressure, and that etching is not limited by chlorination of the surface. The saturated ion current density (and so ion flux) is also nearly independent of pressure. These weak pressure dependences suggest a similar weak dependence of the etch rate on pressure. This is confirmed in Fig. 7; between 0.5 and 10 mTorr, the etch rate is nearly constant.

The dependence of the LD-LIF signal on the laser pulse repetition rate is given in Fig. 8 for Cl_2 pressures of 1.0 and 0.3 mTorr. At 1 mTorr, the signal recorded with the plasma

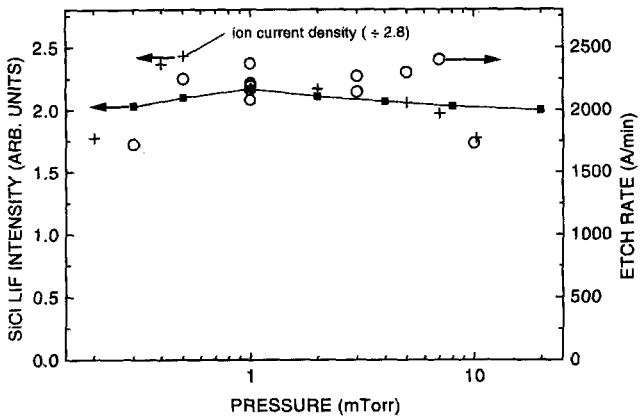

FIG. 7. SiCl LD-LIF signal intensity (■), etch rate (○), and I_{sat} (+) vs P_{Cl_2}. I_{sat} can be obtained by multiplying the left y-axis scale by 2.8 (i.e., I_{sat}=6.2 mA/cm^2 at 1 mTorr). Other conditions are the same as for Fig. 2.

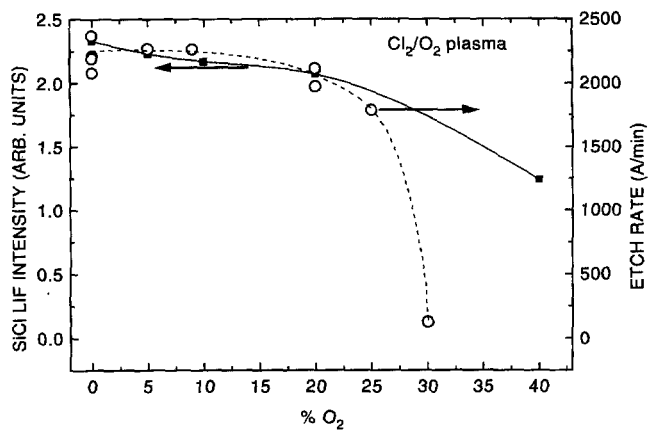

FIG. 9. SiCl LD-LIF signal intensity (■) and etch rate (○) vs %O_2 in Cl_2/O_2 plasmas. Total pressure=1.0 mTorr. Total flow rate=5.5 sccm. Other conditions are the same as for Fig. 2.

on decreases by 30% between 1 and 80 Hz. During plasma etching at 0.3 mTorr, the decrease in intensity with increasing repetition rate is more severe than at 1 mTorr. The signal falls from its limiting value at low repetition rates to $1/e$ of this value at 50 Hz. This corresponds to an apparent first-order rate constant for the formation of the chlorinated layer during plasma etching of about 1.7×10^5 s^{-1} Torr^{-1}.

Oxygen is often added to Cl_2 discharges to improve selectivity with respect to SiO_2 or to reduce undercutting of the mask. The slowing of the SiO_2 etch rate is accompanied by a proportionately smaller reduction in the Si etch rate. This is due to formation of a steady-state coverage of a Si-oxide layer that is competitively being deposited and etched. Oxidation competes with chlorination. LD-LIF measurements were performed to determine the thickness of the $SiCl_{x(ads)}$ layer as a function of oxygen fraction at a constant total pressure of 1 mTorr (Fig. 9). Also plotted in Fig. 9 are the etch rates measured for poly-Si samples. Both the $SiCl_{x(ads)}$ coverage and etch rate exhibit a rapid falloff above ~20% added O_2, suggesting that formation of $SiO_{x(ads)}$ on the surface begins to dominate and hence stop the etching process above 20% O_2.

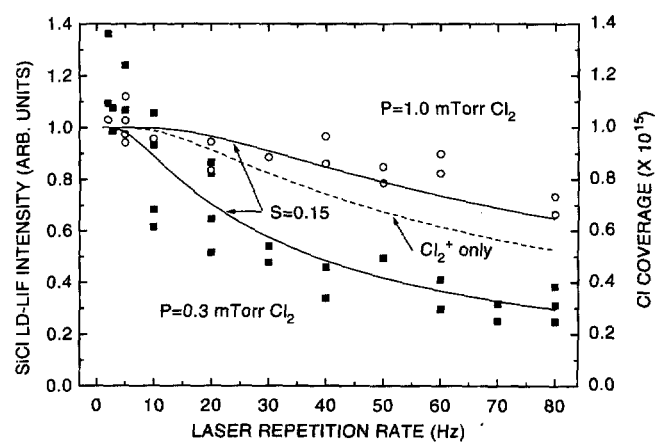

FIG. 8. SiCl LD-LIF signal intensity and Cl coverage vs laser repetition rate for P_{Cl_2}=1.0 (○) and 0.3 (■) mTorr. Other conditions are the same as for Fig. 2. The solid lines are model predictions with Cl_2 as the only source of surface chlorination, and a sticking coefficient of S_{Cl_2}=0.15. The dashed line indicates the Cl coverage from Cl_2^+ impingement alone.

D. Etching mechanisms

Several mechanisms have been proposed for etching of Si in pure Cl_2 plasmas (see, e.g., Refs. 43–45, and references cited therein). All involve ion-bombardment enhancement of the reaction of Cl_2 and Cl with Si to form volatile silicon chloride products. The etching mechanism can be divided into chlorination reactions:

$$Cl_{2(g)}+2Si_{(surf)}\rightarrow 2SiCl_{(ads)}, \quad (2)$$

$$Cl_{(g)}+Si_{(surf,bulk)}\rightarrow SiCl_{(ads)}, \quad (3)$$

$$Cl_{(g)}+SiCl_{(ads)}\rightarrow SiCl_{2(ads)}, \quad (4)$$

$$Cl_2^+ + nSi_{(surf,bulk)}+(2-n)SiCl_{(ads)} \rightarrow nSiCl_{(ads)}+(2-n)SiCl_{2(ads)}, \quad (5)$$

and ion-bombardment stimulated desorption of Si-chloride products:

$$Cl_2^+ + Si_{(bulk)}+SiCl_{x(ads)}\rightarrow SiCl_{y(g)}+SiCl_{z(ads)}, \quad (6)$$

where $n=0$, 1, or 2, and surf and bulk represent a surface or subsurface Si atom, respectively. From mass balance, $x+2=y+z$ if no other Si products (e.g., Si_2Cl_6) desorb and no Cl_2 desorbs or recoils. In fact, some desorption and/or recoiling of Cl_2 is expected. In general, ions in the 20–200 eV energy range are neutralized and dissociated on impact with surfaces.[46] Reaction probabilities (i.e., sticking coefficients) on clean surfaces are typically 0.4–0.8. Sputtering and recoiling of the primary constituents of the ion beam (Cl_2 or possibly Cl atoms) increase with coverage, and so are expected to be more important in reaction (6) than in reaction (5).

We assume that Cl_2 will only chlorinate the surface up to a saturated coverage of $SiCl_{(ads)}$, and ignore small added coverages of higher chlorides ($SiCl_{2(ads)}$ and $SiCl_{3(ads)}$),

found in UHV photoemission studies,[40,42] that could form as a result of Cl_2 impingement. The higher chlorides ($x=2,3$) found in the present study by XPS (Fig. 4) are assumed to be formed through Cl atom and Cl_2^+ impingement. Specific reactions to form $SiCl_{3(ads)}$, analogous to reactions (4) and (5), are left out and are likely to be of only small added importance. We also assume that the predominant ion is Cl_2^+. Strong optical emission was detected from $Cl_2^+(A\ ^2\Pi_u \rightarrow X\ ^2\Pi_g)$ in the 4000–5000 Å region,[24] and no emission from Cl^+ was observed at the expected wavelengths of 3844, 3851, and 3861 Å. Previous optical emission and mass spectrometric studies of a Cl_2 plasma have shown that the appearance of Cl^+ in the plasma is accompanied by strong optical emission at these wavelengths.[47] Even if the predominant ion were in fact Cl^+, the overall conclusions derived below would not be altered. Finally, more than one product species could form; $SiCl_{4(g)}$, $SiCl_{2(g)}$, and $SiCl_{(g)}$ have all been reported as products of ions stimulated etching with a simultaneous flux of Cl_2.[43]

The LD-LIF measurements in Figs. 5, 6, and 7 indicate that chlorination of the surface is only weakly dependent on conditions over the ranges of plasma source powers (0.2–1.0 W/cm^3), substrate dc bias voltages (from 0 to −50 V), and pressures (0.5–10 mTorr) commonly used in high-density plasma etching. This suggests that the surface reaches saturated coverage by chlorine on a time scale that is short compared to the etching rate, and that the etching rate is not limited by the flux of chlorine to the surface, i.e., the sum of the rates of reactions (2)–(5) is fast with respect to reaction (6).

The relative importance of reactions (2)–(4) depends on the percent dissociation of Cl_2, the sticking coefficients of Cl_2 and Cl on Si, and Cl coverage. We have not determined the percent dissociation of Cl_2 in these experiments. Studies carried out mostly at higher pressures and lower plasma densities found that pure Cl_2 discharges are generally rather weakly dissociated.[48–50] No measurements of Cl_2 dissociation have been made in the downstream region of a helical resonator plasma. The closest comparison is with measurements reported by Ono *et al.*[49] downstream from an electron cyclotron resonance (ECR) plasma, where they found ~1% dissociation between 1 and 10 mTorr, with Si etch rates comparable to those in the present study. A low percent dissociation may be expected in the present study because of the high probability for Cl-atom recombination on the stainless-steel walls. If a similar, low percent dissociation occurs downstream from the helical resonator plasma, then chlorination of bare Si sites by Cl_2 would be more important than by Cl unless the sticking coefficient for Cl_2 is much lower than that for Cl. Sticking coefficients have been measured by Kummell and co-workers[51,52] for Cl_2 on clean Si(100) (2×1) and Si(111) (7×7) single-crystal surfaces. At a Cl_2 beam energy of 0.042 eV (corresponding to 500 K) a sticking coefficient of 0.4–0.5 was measured, depending only weakly on crystal orientation and surface temperature (at temperatures relevant to plasma etching, 300–500 K). The sticking coefficient decreases linearly with increasing Cl coverage and reaches zero at saturated coverage. No measurements have been reported for the sticking coefficient of Cl atoms on Si and its dependence on coverage.

From the dependence of the $SiCl_{(g)}$ LD-LIF signal on the laser repetition rate, we can estimate the relative importance of Cl_2, Cl atoms, and Cl_2^+ in chlorinating the surface, and in some cases obtain bounds for sticking coefficients. If we assume Langmuir adsorption with simple first-order kinetics, we can derive the following expression for the dependence of the $SiCl_{(g)}$ LD-LIF signal (I_{SiCl}) on the laser repetition rate:

$$I_{SiCl}=cF\theta_{Cl}^{b}=cF\theta_{Cl}^{\infty}\left(\frac{1-\exp(-\Phi S/r\theta_{Cl}^{\infty})}{1-(1-F)\exp(-\Phi S/r\theta_{Cl}^{\infty})}\right), \quad (7)$$

where F is the fraction of the chlorine coverage that is removed per laser pulse, θ_{Cl}^{b} is the chlorine coverage just before the laser pulse, c is a proportionality constant, S is the sticking coefficient at an adsorption site ($S=0$ is assumed at a fully chlorinated site), r is the laser pulse repetition rate, and θ_{Cl}^{∞} is the saturated coverage of Cl during exposure to the plasma with no laser irradiation (1.0×10^{15} Cl/cm^2, see above). From the data presented in Fig. 3 and other measurements, we determine that $F=0.57$. Φ is the flux of Cl to the surface (e.g., twice the Cl_2 flux if Cl_2 were the only important source of Cl). Equation (7) is valid if the rate of chlorination is fast compared to the rate of formation of new adsorption sites via reaction (6). The term ΦS in Eq. (7) can be expressed as the individual contributions by Cl_2, Cl atoms, and Cl_2^+:

$$\Phi S=2\Phi_{Cl_2}S_{Cl_2}+\Phi_{Cl}S_{Cl}+2\Phi_{Cl_2^+}S_{Cl_2^+}, \quad (8)$$

where Φ and S are fluxes and sticking coefficients for the subscripted species.

In Eqs. (7) and (8) we have assumed a single type of adsorption site. This is an oversimplification for all species, especially for Cl_2, which is expected to have a very low sticking coefficient at coverages greater than $\theta_{Cl}^{\infty}/2$. We also assume that Cl_2^+ requires a site for adsorption. It is more likely that at a bare site, reaction (5) is favored over reaction (6), while on a fully chlorinated site, reaction (6) is more probable than reaction (5). This would make chlorination by Cl_2^+ appear "Langmuir-like," but with a dynamic "saturated coverage" that depends on Cl_2^+ flux and energy.

The Cl_2 flux is given by

$$\Phi_{Cl_2}=n_{Cl_2}v_{Cl_2}/4=\frac{P_{Cl_2}}{\sqrt{2\pi m_{Cl_2}kT_g}}, \quad (9)$$

where P_{Cl_2} is the Cl_2 pressure. The Cl-atom flux can be obtained from an analogous expression with the partial pressure and mass of Cl substituted for Cl_2. From the rotationally resolved N_2 second positive emission spectrum we estimate that the gas temperature, $T_g=500$ K.

The change in Cl coverage in reaction (6) is $z-x(=2-y)$, while in reaction (5) it is 2. If we note that for $y=2$, no change in Cl coverage occurs in reaction (6) and so is equivalent to Cl_2^+ not sticking, then we can write a general expression for an effective fraction of Cl_2^+ that recoils at saturated coverage:

$$f^{\text{eff}}_{Cl_2^+} \geq 1 - Y(E,\theta_{Cl})y/2, \quad (10)$$

where $Y(E,\theta_{Cl})$ is the ion energy and Cl-coverage dependent, chemically enhanced sputtering yield (Si atoms per ion). Negative $f^{\text{eff}}_{Cl_2^+}$ values would indicate a net reduction in Cl coverage because of ion bombardment. Positive values indicate recoiling by Cl_2^+ or sputtering of Cl_2 and Cl atoms from the surface by Cl_2^+.

If we start with the simplest case of 0% Cl atoms, and ignore chlorination by ion bombardment, we then derive $S_{Cl_2}=0.15$ from the fits of Eqs. (7)–(9) to the two sets of data in Fig. 8 (solid lines). This low sticking coefficient, compared to the 0.4–0.5 values reported for clean Si,[51,52] is reasonable, since it is effectively an average sticking coefficient up to a coverage of twice that which is possible with Cl_2 impingement alone. Even with a sticking coefficient as low as 0.15, Cl_2 is important in chlorinating bare Si sites over the pressure range in this study.

Cl atoms and Cl_2^+ are expected to be important in chlorinating Si to roughly double the amount observed with Cl_2 exposure with no plasma. If the gas were only 2% Cl atoms, as found by Ono *et al.*[49] in an electron cyclotron resonance (ECR) plasma, and S_{Cl} were unity, then Cl would contribute only about 10% to the total surface chlorination at 0.3 mTorr, but could contribute 100% of the surface chlorine above several mTorr total pressure. If on the other hand, the gas were >10% Cl atoms, then Cl atoms could be important in the chlorination process even at 0.3 mTorr. Enhanced chlorination by Cl atoms has been reported by Winters and Coburn.[43] In their experiment, the etch rate of Si(111) exposed to Cl atoms and Cl_2 and then bombarded with 2 keV Ar^+ was about three times that for etching with ion bombardment and Cl_2 only. They interpreted this enhancement as evidence for a thicker Si-chloride layer.

Perhaps more important than Cl atoms is chlorination by Cl_2^+. The flux of Cl_2^+ is 3.9×10^{16} cm^{-2} s^{-1}, and is nearly independent of pressure (Fig. 7). At 0.3 mTorr, the flux of Cl_2 is 5.6×10^{16} cm^{-2} s^{-1}. The ion flux is therefore likely to be larger than the Cl atom flux at low pressure. To determine the role of Cl_2^+ in the chlorination process, the chemically enhanced sputtering yields and Si-chloride product stoichiometry must be known.

Sputtering yields in the present study were derived from ion saturation current measurements and etch rate measurements presented in Fig. 6. An expression for the etch rate (ER, Si-atoms/cm^2 s) can be derived from the mechanism presented above, with reaction (6) as the rate-limiting step

$$ER = \Phi_{Cl_2^+}[Y(E,\theta_{Cl})] \propto (\theta_{Cl})(\Phi_{Cl_2^+})[Y(E)], \quad (11)$$

where $Y(E)$ is the yield at a nominal, constant Cl-coverage.

The ion energy (E) was assumed to be equal to the plasma potential (50 V) minus the dc bias voltage of the substrate holder. The yields, plotted versu $\sqrt{E}$ in Fig. 10, range from 0.38 at 50 eV to 0.60 at 125 eV. Apparently, sputtering yields have not been reported for Cl_2^+ at the low energies of interest in this study. Oostra *et al.*[53] have reported sputtering yields for Si(111) by Ar^+ at a Cl_2 flux of 1×10^{17} cm^{-2} s^{-1}, high enough to achieve saturated coverage. They found an approximate $\sqrt{E}$ dependence between 1000 eV (yield=3.0) and 100 eV (yield=0.75), and a more pronounced decrease in the yield (=0.25) at 50 eV.

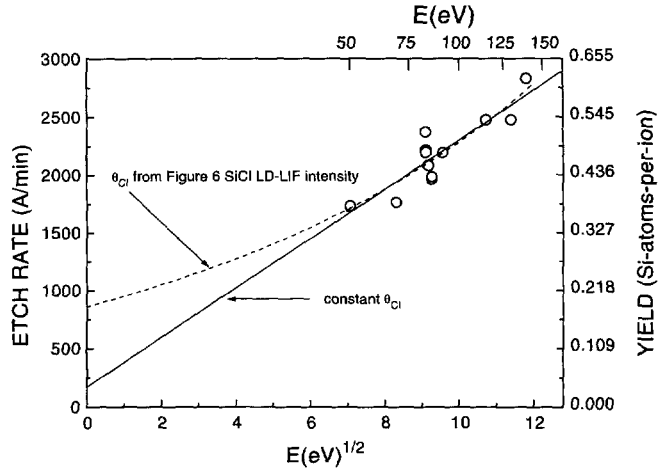

FIG. 10. Si etch rates and sputtering yields (Si-atoms-per-ion) vs ion energy. The dashed curve is a least-squares fit to Eqs. (11) and (12), where θ_{Cl} is assumed to be proportional to the SiCl LD-LIF signal shown in Fig. 6. The solid curve is a linear least-squares fit, assuming that the sputtering process does not depend on Cl coverage near saturated coverage.

If we use a value of $Y(E,\theta_{Cl})=0.5$ (at a bias voltage V dc=−36) and assume an average stoichiometry of $SiCl_{2(g)}$ for the etch product, then from Eq. (10) $f^{\text{eff}}_{Cl_2^+}=0.5$. This high value for $f^{\text{eff}}_{Cl_2^+}$ indicates that some Cl_2 desorbs or recoils during ion bombardment, and/or that the average product is more highly chlorinated than $SiCl_{2(g)}$. Assuming the latter is not the case and that sputtering does not occur at a bare Si-site substituting $S_{Cl_2^+}=1-f^{\text{eff}}_2$ into Eqs. (7) and (8) and setting S_{Cl_2} and $S_{Cl}=0$ we can estimate the importance of Cl_2^+ alone to the chlorination process. This calculation is included in Fig. 8. The computed Cl coverages exceed measurements at 0.3 mTorr and are nearly equal to those observed at 1.0 mTorr, indicating that Cl_2^+ alone could be sufficient for chlorinating the surface to near saturated coverage in the plasma.

A $\sqrt{E}$ dependence for sputtering yields is usually interpreted in terms of a collision-cascade mechanism. On the other hand, in a more recent study by Oostra *et al.*[54] the velocity distributions of products of low-energy ion-assisted etching were presented as support for a local hot-spot model, i.e., single ions transiently heat a small region and promote thermal reactions that lead to product desorption. Steinbruchel has reported an expression for the energy dependence of ion-enhanced chemical sputtering yield by a collision-cascade process[55]

$$Y(E)=A(E^{1/2}-E^{1/2}_{th}), \quad (12)$$

where $E^{1/2}_{th}$ is a threshold energy and A is a proportionality constant. Using data of Oostra *et al.*[53] Steinbruchel[55] estimated $E^{1/2}_{th}$ of 17 eV for Ar^+ sputtering of Si in the presence of Cl_2. The threshold energy for a collision cascade, *physical* sputtering process has a complicated dependence on the masses of the projectile ion and target atoms.[56] When the

masses of the ion and substrate atoms are similar, E_{th} for a given substrate is approximately proportional to the square root of the mass of the ion. Consequently, the value for E_{th} for Cl_2^+ might be expected to be 30% higher than that for Ar^+. On the other hand, since Cl_2 will dissociate on impact, the mass dependence may approach that of Cl^+ (and Ar^+). In addition, the formation of SiCl bonds lowers the surface binding energy[41] (U_s in physical sputtering collision cascade theory), and correspondingly E_{th} may be still lower.

It is unclear how well Eq. (12) describes the low energy ion dependence in the local hot-spot model proposed by Oostra *et al.*[54] Nonetheless, we can compare the predictions of Eq. (12) with our measured etch rates. The dashed curve in Fig. 10 represents a least-squares fit of Eqs. (11) and (12) to the etch rate data, with relative values of θ_{Cl} taken from the linear fit to the $SiCl_{(g)}$ LD-LIF measurements in Fig. 6. The model predicts a negative E_{th} and is therefore unreasonable. If on the other hand $Y(E, \theta_{Cl})$ deviated from Eq. (11) and the etch rate were independent of θ_{Cl} near saturated coverage, then the sputtering yields would follow a $\sqrt{E}$ dependence with a threshold energy near zero (solid line, linear least-squares fit in Fig. 10).

The low sputtering yields presented in Fig. 10 and the importance of Cl_2^+ in forming the saturated chloride layer indicate that anisotropic etching in low pressure, high charge density plasmas proceeds by a different mechanism than occurs in reactive ion etching (RIE). In the RIE process, ion energies are several hundred eV and yields of several Si atoms-per-ion require chlorination predominantly by impinging neutral species. In high density plasmas on the other hand, the high flux of low energy ions provides enough chlorine to form $SiCl_{4(g)}$ at the observed etch rates, although the major product in likely $SiCl_{2(g)}$ and possibly some $SiCl_{(g)}$.[43] Therefore, one expects a collision cascade mechanism or a local hot-spot model for anisotropic etching to be complicated by the role of dissociative chemisorption of Cl_2^+.

Finally, the dependence of the etch rate on the percent added O_2 (Fig. 9) indicates that the etch rate falls more abruptly than does the fractional coverage of Cl. This suggests that formation of SiO_xCl_y species on the surface are important in suppressing etching of Si, and that the surface need not be converted completely to SiO_2.

IV. CONCLUSIONS

Laser-induced desorption, combined with laser-induced fluorescence detection of $SiCl_{(g)}$, has been used to study the $SiCl_{x(ads)}$ layer present during etching of Si in a high density, low pressure helical resonator plasma of pure Cl_2 and mixtures of Cl_2 and O_2. The $SiCl_{x(ads)}$ layer present during etching contains about twice as much Cl (mainly as $SiCl_{2(ads)}$ and $SiCl_{3(ads)}$) as the saturated layer formed by exposing Si to Cl_2 in the absence of a plasma. Chlorination of the surface during etching is attributed to Cl_2 impingement up to a coverage of 5×10^{14} Cl/cm^2, and to Cl-atom impingement and Cl_2^+ dissociative chemisorption up to a saturated coverage of 1×10^{15} Cl/cm^2. At pressures above ~0.5 mTorr, the $SiCl_{x(ads)}$ layer reaches saturated coverage on a time scale that is short compared to the etch rate. Up to the highest powers and dc bias voltages investigated, no falloff was observed in $SiCl_{x(ads)}$ thickness, indicating that ion flux still limits the rate of desorption of etch products, and therefore the etch rate, even in these low pressure, high-charge density plasmas. The ion-enhanced etching process at the lowest ion energies investigated has a threshold energy near zero. The low sputtering yields (0.38 and 0.60 Si atoms-per-ion at 50 and 125 eV, respectively) suggests that a substantial amount of the chlorine required to form volatile $SiCl_x(g)$ products is supplied by the impinging ions, unlike the mechanism in the higher ion energy, reactive ion etching process.

The thickness of the $SiCl_{x(ads)}$ layer does not decrease appreciably after the plasma is extinguished and the gas pumped away. Consequently, post-etching surface analysis measurements on samples that are transferred under UHV to the analysis chamber provides information on the surface that was present during etching.

ACKNOWLEDGMENTS

Acknowledgment is made to the donors of the Petroleum Research Fund, administrated by the ACS, for partial support of I. P. Herman's involvement in this research. The authors also thank C. P. Chang for technical discussions.

[1]B. Drevillon, Thin Solid Films **163**, 157 (1988).
[2]R. W. Collins and B. Y. Yang, J. Vac. Sci. Technol. B **7**, 1155 (1989).
[3]D. E. Aspnes, W. E. Quinn, and S. Gregory, Appl. Phys. Lett. **56**, 2569 (1990).
[4]S. W. Downey, A. Mitchell, and R. A. Gottscho, J. Appl. Phys. **63**, 5280 (1988).
[5]E. Yoon, R. A. Gottscho, V. M. Donnelly, and W. S. Hobson, J. Vac. Sci. Technol. B **10**, 2197 (1992).
[6]E. S. Aydil, Z. H. Zhou, K. P. Giapis, J. A. Gregus, Y. J. Chabal, and R. A. Gottscho, Appl. Phys. Lett. **62**, 3156 (1993).
[7]J. L. Vossen, J. H. Thomas III, J.-S. Maa, O. R. Mesker, and G. D. Fowler, J. Vac. Sci. Technol. A **1**, 1452 (1983).
[8]J. H. Thomas III and J.-S. Maa, Appl. Phys. Lett. **43**, 859 (1983).
[9]M. Sekine, T. Arikado, H. Okano, and Y. Horiike, Proceedings of the Symposium on Dry Processes, Tokyo, 1986 (unpublished), p. 42.
[10]K. Hirobe, K. Kawamura, and K. Norjiri, J. Vac. Sci. Technol. B **5**, 594 (1987).
[11]D. A. Jackel, C. Mazure, H. J. Barth, H. Cerva, and W. Hosler, J. Vac. Sci. Technol. B **7**, 505 (1989).
[12]G. S. Oehrlein, K. K. Chan, and M. A. Jaso, J. Appl. Phys. **64**, 2399 (1988).
[13]G. S. Oehrlein, A. A. Bright, and S. W. Robey, J. Vac. Sci. Technol. A **6**, 1989 (1988).
[14]G. S. Oehrlein, J. F. Rembetski, and E. H. Payne, J. Vac. Sci. Technol. B **8**, 1199 (1990).
[15]G. S. Oehrlein, K. K. Chan, M. A. Jaso, and G. W. Rubloff, J. Vac. Sci. Technol. A **7**, 1030 (1989).
[16](a) K. V. Guinn and V. M. Donnelly, J. Appl. Phys. **75**, 2227 (1994); (b) K. V. Guinn, C. C. Cheng, and V. M. Donnelly, J. Vac. Sci. Technol. (to be published).
[17]I. P. Herman, K. V. Guinn, C. C. Cheng, and V. M. Donnelly, Phys. Rev. Lett. **72**, 2801 (1994).
[18]J. A. McCaulley, V. R. McCrary, and V. M. Donnelly, J. Phys. Chem. **93**, 1148 (1989).
[19]J. A. McCaulley and V. M. Donnelly, J. Chem. Phys. **91**, 4330 (1989).
[20]J. A. McCaulley, R. J. Shul, and V. M. Donnelly, J. Vac. Sci. Technol. A **9**, 2872 (1991).
[21]J. M. Cook, D. E. Ibbotson, and D. L. Flamm, J. Vac. Sci. Technol. B **8**, 1 (1990).
[22]J. M. Cook, D. E. Ibbotson, P. D. Foo, and D. L. Flamm, J. Vac. Sci. Technol. A **8**, 1820 (1990).
[23]D. E. Ibbotson, J. M. Cook, and C-P. Chang, *Proceedings of the 12th Symposium on Dry Process* (IEE, Japan, Tokyo, 1990), p. 93.
[24]K. P. Huber and G. Herzberg, *Constants of Diatomic Molecules* (Van Nostrand Reinhold, New York, 1979).

[25]D. M. Phillips, J. Phys. D **9**, 507 (1975).
[26]R. A. Porter and W. R. Harshbarger, J. Electrochem. Soc. **126**, 460 (1979).
[27]G. P. Davis and R. A. Gottscho, J. Appl. Phys. **54**, 3080 (1983).
[28]S. Singleton, K. G. McKendrick, R. A. Copeland, and J. B. Jeffries, J. Phys. Chem. **96**, 9703 (1992).
[29]J. B. Jeffries, J. Chem. Phys. **95**, 1628 (1991).
[30]*Spectroscopic Data*, Heteronuclear Diatomic Molecules Vol. I, edited by S. N. Suchard (IFI Plenum, New York, 1975), part B, p. 992.
[31]A. Aliouchouche, J. Boulmer, B. Bourguignon, J.-P. Budin, D. Debarre, and A. Desmur, Appl. Surf. Sci. **69**, 52 (1993).
[32]J. Boulmer, B. Bourguignon, J.-P. Budin, and D. Debarre, Appl. Surf. Sci. **43**, 424 (1989).
[33]J. Boulmer, B. Bourguignon, J.-P. Budin, and D. Debarre, Chemitronics **4**, 165 (1989).
[34]J. Boulmer, B. Bourguignon, J.-P. Budin, D. Debarre, and A. Desmur, J. Vac. Sci. Technol. A **9**, 2923 (1991).
[35]R. DeJonge, J. Majoor, K. Benoist, and D. DeVries, Europhys. Lett. **2**, 843 (1986).
[36]G. Meijer, W. Ubachs, J. J. ter Meulen, and A. Dymanus, Chem. Phys. Lett. **139**, 603 (1987).
[37]P. L. Cowan and J. A. Golovchenko, J. Vac. Sci. Technol. **17**, 1197 (1980).
[38]C. C. Cheng, Q. Gao, W. J. Choyke, and J. T. Yates, Jr., Phys. Rev. B **46**, 12 810 (1992).
[39]Q. Gao, C. C. Cheng, P. J. Chen, W. J. Choyke, and J. T. Yates, Jr., J. Chem. Phys. **98**, 8308 (1993).
[40]T. D. Durbin, W. C. Simpson, V. Chakarian, D. K. Shuh, P. R. Varekamp, C. W. Lo, and J. Yarmoff, Surf. Sci. (in press).
[41]H. Feil, J. Dieleman, and B. J. Garrison, J. Appl. Phys. **74**, 1303 (1993).
[42]L. J. Whitman, S. A. Joyce, J. A. Yarmoff, F. R. McFeely, and L. J. Terminello, Surf. Sci. **232**, 297 (1990).
[43]H. F. Winters and J. W. Coburn, Surf. Sci. Rep. **14**, 161 (1992).
[44]D. L. Flamm, V. M. Donnelly, and D. E. Ibbotson, in *VLSI Electronics Microstructure Science* (Academic, Orlando, 1984), pp. 189–251.
[45]A. Manenschijn, E. van der Drift, G. C. A. M. Janssen, and S. Radelaar, J. Appl. Phys. **69**, 7996 (1991).
[46]S. R. Kasi, H. Kang, C. S. Sass, and J. W. Rabalais, Surf. Sci. **10**, 1 (1989).
[47]V. M. Donnelly and D. L. Flamm, J. Appl. Phys. **58**, 2135 (1985).
[48]J. Wormholdt, A. C. Stanton, A. D. Richards, and H. H. Sawin, J. Appl. Phys. **61**, 142 (1987).
[49]K. Ono, T. Oomori, M. Tuda, and K. Namba, J. Vac. Sci. Technol. A **10**, 1071 (1992).
[50]E. S. Aydil and D. J. Economou, J. Electrochem. Soc. **139**, 1406 (1992).
[51]D. J. D. Sullivan, H. C. Flaum, and A. C. Kummel, J. Phys. Chem. **97**, 12 051 (1994).
[52]H. C. Flaum, D. J. D. Sullivan, and A. C. Kummel, J. Phys. Chem. **98**, 1719 (1994).
[53]D. J. Oostra, R. P. van Ingen, A. Haring, and A. E. de Vries, Appl. Phys. Lett. **50**, 1506 (1987).
[54]D. J. Oostra, A. Haring, R. P. van Ingen, and A. E. de Vries, J. Appl. Phys. **64**, 315 (1988).
[55]C. Steinbruchel, Appl. Phys. Lett. **55**, 1960 (1989).
[56]Y. Yamamura and J. Bohdansky, Vacuum **35**, 561 (1985).